T. Bierkandt, T.Kasper, E. Akyildiz, A. Lucassen, P. Oßwald, M. Köhler, P. Hemberger, Flame structure of a low-pressure, laminar premixed and lightly sooting acetylene flame and the effect of ethanol addition, Proc. Combust. Inst. 35 (2015) 803-811.

The original publication is available at www.elsevier.com

doi 10.1016/j.proci.2014.05.094

Flame structure of a low-pressure, laminar premixed and lightly sooting acetylene flame and the effect of ethanol addition

T. Bierkandt[a]. T.Kasper[a]*, E. Akyildiz[a], A. Lucassen[b], P. Oßwald[c], M. Köhler[c], P. Hemberger[d]

[a] *University of Duisburg-Essen, Germany*
[b] *Sandia National Laboratories, Livermore, California, USA*
[c] *DLR – Institute of Combustion Technology, Stuttgart 70569, Germany*
[d] *Molecular Dynamics Group, Swiss Light Source, Paul Scherrer Institut, Villigen CH 5232, Switzerland*

Corresponding Author: T. Kasper, Thermodynamics, Lotharstr. 1, 47057 Duisburg, Germany
phone: +49-203-379-1854, fax: +49-203-379-1250
email: tina.kasper@uni-due.de

Colloquium Topic Area: Laminar Flames

Part	Method	# words
Main text	Microsoft Word 2010 word count	3321
Equations	(0) lines × 7.6 words/line	0
References	(43 + 2) × 2.3 lines/ref × 7.6 words/line	787
Tables	[(0+2)*1 + (+2)*1 + (+2)] × 7.6 words/line	0
Figure 1	[(91 mm + 10 mm) × 2.2 words/mm] + 31	253
Figure 2	[(96 mm + 10 mm) × 2.2 words/mm] + 28	261
Figure 3	[(56 mm + 10 mm) × 2.2 words/mm] + 24	169
Figure 4	[(57 mm + 10 mm) × 2.2 words/mm] + 28	175
Figure 5	[(57 mm + 10 mm) × 2.2 words/mm] + 14	161
Figure 6	[(57 mm + 10 mm) × 2.2 words/mm] + 21	168
Figure 7	[(57 mm + 10 mm) × 2.2 words/mm] + 21	168
Figure 8	[(56 mm + 10 mm) × 2.2 words/mm] + 23	168
Figure 9	[(56 mm + 10 mm) × 2.2 words/mm] + 24	169
Total		**5800**

Supplemental material has been included in the submission of this paper.

Submitted to the 35th International Symposium on Combustion, San Francisco, CA, August 3-8, 2014.

Flame structure of a low-pressure, laminar premixed and lightly sooting acetylene flame and the effect of ethanol addition

T. Bierkandt, T.Kasper, E. Akyildiz, A. Lucassen, P. Oßwald, M. Köhler, P. Hemberger

Abstract

The flame structure of a fuel-rich (ϕ = 2.4), laminar premixed, and lightly sooting acetylene flame at 40 mbar and the influence of ethanol addition on the species pool was investigated. Special emphasis was put on the analysis of important soot precursors like propargyl, benzene, and the polyynes. The mole fractions of more than 50 stable and radical species up to *m/z*=170 are obtained experimentally in the flames by molecular-beam mass spectrometry (MBMS) in combination with single-photon ionization (SPI) by vacuum ultraviolet (VUV) radiation from the Advanced Light Source (ALS) in Berkeley, CA, USA. For the neat acetylene flame, successful measurements were performed with a combination of MBMS and imaging photoelectron photoion coincidence spectrometry (iPEPICO) at the VUV beamline at the Swiss Light Source (SLS) in Villigen, Switzerland and add additional species information to the data set. Some interesting isomers (C_3H_2, C_4H_5, C_4H_2O) can be clearly identified by comparison of measured photoionization efficiency (PIE) curves or threshold photoelectron (TPE) spectra with Franck-Condon simulations or literature spectra, respectively. Because of apparatus improvements, the chemical resolution in this study goes beyond prior work and provides a high-quality data set for the development of reaction mechanisms at fuel-rich, low-pressure conditions.

Keywords: acetylene flame structure; ethanol addition; VUV photoionization; threshold photoelectron spectroscopy; soot precursors

1. Introduction

In times of increasing oil scarcity and rising fuel prices, the share of biofuels as a fuel substitute or additive grows continuously and bioethanol is one of the main fossil fuel substitutes [1]. Different fuels like acetylene [2], ethylene [3], benzene [4] and commercial gasoline [5] were used in previous studies under various conditions to investigate the effect of ethanol addition under fuel-rich conditions, which resulted each time in a diminution of the production of soot compared to the combustion of neat fuel. Here, the species C_2H_2 (acetylene), C_3H_3 (propargyl radical), C_3H_5 (allyl radical), and C_6H_6 (benzene) are of particular importance for the formation of polycyclic aromatic hydrocarbons (PAHs). The PAHs themselves play a key role for the formation of soot and their formation is described by the fuel-independent H-abstraction-C_2H_2-addition (HACA) mechanism according to Frenklach et al. [6]. Addition of acetylene to an aromatic radical leads to higher aromatics like naphthalene or phenanthrene. Acetylene itself is in the exhaust gas of fuel-rich flames the dominant hydrocarbon and therefore the most likely growth component. Depending on the fuel, other reactions of small hydrocarbons with aromatic compounds must be considered [7]. Polyynes ($C_{2n}H_2$, $n\geq2$), which are linear-chain carbon molecules, have a high reactivity in polymerization reactions and are associated with soot [8,9].

Alternative oxygenated fuels like ethanol can provide, under certain conditions, a positive life-cycle assessment and thus environmental benefits particularly with regards to greenhouse-gas emissions reduction. Unfortunately, increased emissions of other toxic species like aldehydes are observed [10]. To control pollutant emissions, the corresponding chemical processes involved in combustion must be studied in well-controlled fundamental laboratory experiments. An established technique for species analysis in model flames is molecular-beam mass spectrometry.

Numerous fuel-rich acetylene flames with different stoichiometries have been investigated previously by molecular-beam mass spectrometry in combination with electron-impact ionization [11-14] but to our knowledge only twice with photoionization [15,16]. The experimental results can be used to improve kinetic models particularly the modeling of soot precursor and soot formation. Experimental data are compared to a state-of-the-art model to demonstrate very satisfactory agreement, but efforts to gain fundamental new insights on acetylene chemistry from the comparison go beyond the scope of this experimental work. The fuel-rich acetylene flames considered here demonstrate the resolution of the new time-of-flight mass spectrometer at the ALS and the first results from a new flame system at the SLS. Furthermore, ethanol addition to the neat acetylene flame provides initial insights into the chemical changes induced in the intermediate species pool for a fuel with the one of the highest sooting propensities.

2. Experiment

We measured two fuel-rich flames with stoichiometries of ϕ = 2.40 at 40 mbar. The acetylene flame had a cold-flow composition of $C_2H_2/O_2/Ar$ = 0.98/1.02/2.00 and a C/O ratio of 0.96. For the blended flame 10% of the acetylene is substituted by ethanol while stoichiometry, dilution and cold gas velocity are kept constant. The conditions are as follows: $C_2H_2/C_2H_5OH/O_2/Ar$ = 0.873/0.097/1.03/2.00 and C/O ratio of 0.90. The total gas flow for both flames was 4 slm. The flames are stabilized on 6.00-cm-diameter water-cooled McKenna burners. Gases are regulated by calibrated mass flow controllers. Ethanol is metered liquid, vaporized [17], and added to the premixed gas stream at the ALS setup.

The MBMS setup at the Chemical Dynamics Beamline 9.02 at the ALS and the VUV beamline at the SLS are comparable and described in detail in [18] and [19], respectively. In addition, the mass spectrometer of the ALS setup has been upgraded and now features a new time-of-flight (TOF) mass spectrometer (Kaesdorf) with mass resolution of $m/\Delta m \approx 3500$, which allows separation of nearly identical masses; e.g., CO and C_2H_4. Mass resolution at the SLS is $m/\Delta m \approx 200$. The iPEPICO detection scheme at the SLS allows the simultaneous measurement of photoionization mass spectra and velocity map images of electrons in coincidence, permitting to measure mass selected threshold photoelectron spectra (ms-TPES). Details can be found in [20,21]. The ms-TPES reflect unique state-specific transitions and yield a fingerprint of the molecules with a resolution that surpasses the resolution of photoionization efficiency curves measured at the ALS or SLS. Consequently, species identification of isomeric species can be performed with higher confidence at the SLS. In principle, the instrument at the SLS can provide an independent quantitative data set [19] in future work, but it was used here to supplement speciation information.

In order to achieve assignment of the different species and to create concentration profiles, two different measurements were conducted: A burner scan, where the ionization energy is constant and the burner position is changed, and an energy scan, where the position of the burner is stationary and the ionization energy is varied.

Procedures for the evaluation of species mole fractions follow Cool et al. [22]. The data-reduction procedures for the ALS system were further refined and a summary, including error discussion, can be found in [17]. Data reduction of the SLS mass spectra follows the same logic, and a description of the appropriate modifications can be found in [19].

3. Results and Discussion

Overall, we detected more than 50 intermediate species in the fuel-rich acetylene flame with the new mass spectrometer at the ALS and calculated their mole fraction profiles. This number of species is similar to [15]. Table S1 in the

supplemental material gives details of the measured species at the ALS in the acetylene flame as well as the flame blended with ethanol and lists their maximum mole fractions with the corresponding burner positions.

It is striking that for the intermediates with the largest concentrations, the maximum mole fractions in the mixed flame are lower than in the neat acetylene flame. This is especially true for the main soot precursors propargyl (1.18 times lower) and benzene (1.25 times lower), the polyynes, and some other hydrocarbons like C_6H_4 or C_3H_2. In contrast, the maximum mole fractions of oxygenated species like ketene (C_2H_2O) or acetaldehyde (C_2H_4O) and also the concentrations of allyl and methyl radicals are lower in the neat flame. These observations suggest changes in flame chemistry which go beyond the 10% replacement effect expected for a 10% replacement of acetylene fuel with ethanol.

Major species

In Fig. 1, the experimental mole fraction profiles of the major species in the acetylene flame and the blended flame with 10 % ethanol are presented and compared with the modeling results. Furthermore, the temperature profiles, which were used for the modeling, are mapped.

The experimental temperature profiles were determined from the temperature dependence of the sampling rate through the quartz nozzle, which means that the shape of the profile is derived from the argon mole fraction. The determination of a temperature profile in this way is afflicted with larger errors than a direct measurement but it has been shown that this procedure is a useful approximation for modeling MBMS data [23] that eliminates the need to shift simulated profiles. The temperature in the exhaust gas was set to 2000 K for the pure acetylene flame based on similar flames [12,15]. Also for the C_2H_2/C_2H_5OH flame, the exhaust gas temperature was set to be 2000 K because of the nearly identical adiabatic temperature in both flames.

Finally, the experimental data for the reactants (C_2H_2, O_2, Ar, C_2H_5OH) and major products (H_2, H_2O, CO, CO_2) match in good approximation the simulated mole fractions predicted by the mechanism of Miller [24,25]. Agreement for H_2 and H_2O mole fractions is nearly perfect and is within 15% for CO and CO_2. Deviations are within the error limits of the main-species mole fractions (10-15%) For the acetylene flame, oxygen and fuel are consumed more rapidly so that the main reaction zone is closer to the burner (about 1 mm), and H_2 and H_2O exhaust concentrations are slightly lower than for the ethanol-doped flame. Acetylene is the most abundant hydrocarbon in the exhaust gas (similar concentration as CO_2) and has a major influence on the formation of soot precursors.

Similar results are observed in the comparison of the experimental data and the calculated mole fractions for the major species in the acetylene flame measured at the SLS (Fig. S1, supplemental material). However, the concentration profile of H_2 is somewhat lower and the H_2O higher compared to the data obtained by PI-MBMS at the ALS and the simulation. Data-reduction procedures for the SLS data are still in an early stage of development and have, for example, not taken experimental mass-discrimination-correction factors into account, which can account for some of the deviations. Overall, the experimental data for the pure acetylene flame give a satisfactorily consistent overview of the flame structure even though they were measured with different MBMS systems.

Combustion intermediate species

The propargyl radical (C_3H_3), as a major benzene precursor molecule, is the most important species for soot formation and can be found under fuel-rich conditions with typical mole fractions of 10^{-3}-10^{-4}. Its formation is based on the reaction of acetylene with singlet CH_2 and to a minor extent with triplet CH_2 [16,26]. The measured signal intensity for m/z = 39 from the energy scans fits the PIE curve from [27] very well for both systems (Fig. 2). Furthermore, the TPE spectrum of the propargyl radical recorded at 3.46 mm above the burner surface fits the intensity and position of the adiabatic ionization energy at 8.70 eV obtained from a Franck-Condon simulation [28] very well and is also in coincidence with previous experimental data [29]. Concentration of propargyl radicals directly affects the formation of benzene and phenyl due to the recombination reaction ($C_3H_3 + C_3H_3 = C_6H_6$ or $C_6H_5 + H$) and reaction with the allyl radical (C_3H_5). Both radical recombinations are important for the formation of C_6 aromatic hydrocarbons and thus for the formation of PAHs [30].

In contrast, benzene formation through C_2H_2 and *n*-C_4H_3 or *n*-C_4H_5 [31] plays no significant role for the benzene production in acetylene flames [26] because of the low concentration of the *n*-isomers in comparison to the resonantly stabilized *i*-isomers [18]. Our measurements confirm that the dominant species in a fuel-rich acetylene flame is *i*-C_4H_3 for m/z = 51. For m/z = 53 we could identify *i*-C_4H_5 clearly. Distinction between CH_3CCCH_2 and CH_3CHCCH was not possible but a comparison of PIE spectra from measurements at the SLS system with previous work by Hansen et al. [32] shows, however, that either or both of these species are present as shown in Fig. 3.

Because the propargyl mole fraction is lower in the ethanol-doped than in the neat flame, the mole fraction of benzene should also be lowered by the addition of ethanol. The experimental data (1.25 times lower) as well as the modeling results (1.74 times lower) confirm this effect. Benzene is the most abundant isomer in the acetylene flames, but fulvene can also be clearly identified by its onset near 8.36 eV in the PIE spectrum. Its concentration was calculated to be about 7.5 times lower than benzene. Figure 4 demonstrates how well the integrated signal intensities of m/z = 78 from the

energy scan of the neat acetylene flame match the literature cross sections of fulvene [33] and the weighted sum of the fulvene and benzene [34] cross sections, respectively. The mole fraction profiles of some other aromatics (benzyne, toluene, phenol, phenylacetylene, naphthalene and indene) can also be obtained from the ALS data. Through recombination, the cyclopentadienyl radical (C_5H_5) can lead directly to the formation of higher PAHs like $C_{10}H_8$ whereas formation of naphthalene is favored at low temperature and of fulvalene at high temperature [35]. PAHs with three or more condensed aromatic rings (e.g., phenanthrene and anthracene) could not be detected. The lack of higher PAHs in this slightly sooting flame leads to the assumption that the concentrations of these species are under the detection limit or they play only a minor role for the formation of soot in acetylene flames and the "acetylene route" [36], which indicates the formation of soot aerosols by chemical condensation of polyynes at high temperatures, is more favored.

The allyl radical could be detected in low concentration and can be clearly identified with the help of the threshold photoelectron spectrum. Figure 5 shows the TPES obtained from the measurements at the SLS in comparison with a spectra measured by Schüßler et al. [37]. Both peaks, the vertical ionization energy at 8.133 eV and the cationic CCC bending mode ν_7^+ at 8.185 eV are in good approximation with our data (8.139 and 8.189 eV, respectively). Other C_3H_5 isomers (e.g. 2-propenyl or cyclopropyl radical) could not be observed. The experimental peak mole fraction is 1.35 times higher in the flame blended with ethanol. This increase is in agreement with the modeling result, which also predicts a small increase of the peak concentration by the addition of ethanol. The main production path to form allyl is the reaction of C_2H_3 with the methyl radical [26]. The fact that the allyl radical concentration is higher in the ethanol-blended flame implies another route for its formation. The experimental as well as the simulated results show that the concentration of CH_3 is higher for the flame with ethanol (about 1.45 times). The ethane concentration also increases through methyl radical recombination.

The C_3H_2 isomers are important for PAH formation because they are in equilibrium with propargyl and form C_4H_5 by the reaction with methyl. They were studied in detail by Taatjes et al. [38], who observed propargylene and cyclopropenylidene in a rich cyclopentene flame. Figure 6 shows the PIE curve at 6.5 mm above the burner surface for the present fuel-rich acetylene flame. The curve has an onset at 8.9 eV, which coincides with the ionization potential of triplet propargylene. Comparison of the measured PIE spectrum with a Franck-Condon simulation of photoionization from triplet propargylene at 300 K from [38] reveals another C_3H_2 isomer with an IP about 9.15 eV. Hence, the best fit to the measured PIE spectrum is the sum of Franck-Condon simulations for photoionization from triplet propargylene (60%) and cyclopropenylidene (40%).

Polyacetylenes, so-called polyynes, are well-known [8] to be associated with soot. They appear at the end of the reaction zone and their chain growth occurs through reaction with acetylene ($C_{2n}H + C_2H_2 = C_{2n+2}H_2 + H$) or its radical C_2H

($C_{2n}H_2 + C_2H = C_{2n+2}H_2 + H$) until they reach their maximum stable length. The thermodynamic stability of polyynes increases with higher temperatures whereas the stability of other hydrocarbons decreases [36]. Furthermore, large polyyne radicals can react with each other. We found polyynes up to $C_{14}H_2$ in the neat acetylene flame and with lower concentrations in the ethanol-doped flame as Fig. 7 shows. Their ionization energy decrease monotonically with their chain length and can be found for C_4H_2, C_6H_2, and C_8H_2 in the NIST database. In recent studies, ionization energies for polyynes up to $C_{18}H_2$ were experimentally determined or calculated [15,39,40]. These values are in good agreement with our results as shown in (Table S2, supplemental material). In Fig. 7 the maximum mole fractions for the polyynes from C_4H_2 up to $C_{14}H_2$ are plotted in logarithmic scale against the number of carbon atoms in the molecule and show that the peak concentrations nearly exponentially decrease with the chain length of the polyynes. In other words, the concentration ratio of $C_{2n}H_2/C_{2n-2}H_2$ should be constant, as previously concluded by Li et al. [15]. These observations can help to improve existing models to consider the formation of higher polyynes. Especially, the small polyynes diacetylene (C_4H_2) and hexatriyne (C_6H_2) are detectable in higher concentrations in the exhaust gas zone than all other intermediate species. This observation is due to the fact that acetylene itself is not consumed completely under fuel-rich conditions and still promotes the formation of the polyynes. The experimental data and the modeling results indicate a decrease of the mole fractions of polyynes for the ethanol-doped flame in agreement with the trend for C_4H_2 and C_6H_2 in the simulation. The model does not consider the formation of higher polyynes than C_6H_2.

Similar conclusions as for the polyynes can derived for the polyynic compounds C_nH_4 ($n \geq 4$) which were detected up to $C_{11}H_4$. To our knowledge, $C_{11}H_4$ was not detected before in an acetylene flame. Again, there is an almost exponential correlation between the maximum mole fractions of the different C_nH_4 species as shown in Fig. 7. If C_4H_4 is omitted from the trend, a linear correlation describes the diminution of the concentration for the other polyynic compounds even better. However, it must be considered that for large polyynic C_nH_4 intermediates, no measured photoionization cross sections are available and the error of the concentrations can be large. Overall, both the concentration of polyynes and polyynic intermediates decrease with the substitution of 10% acetylene by ethanol. From Fig. 7 it follows that the relative decrease in mole fraction increases with the number of carbon atoms and that the mole fractions of large polyyne and polyynic C_nH_4 are affected stronger by the addition of ethanol.

In previous measurements of rich acetylene flames [12,15], the signal of m/z = 66 was supposed to belong to C_5H_6. However, the existence of C_4H_2O could not be excluded [13]. Here, we observed two peaks in the mass spectra for mass 66 with peak maxima at different burner positions clearly identified as C_5H_6 and C_4H_2O. A more detailed identification of isomers can be done by PIE spectra. Figure 8 gives a comparison of the measured PIE curve for C_5H_6 with the Franck-Condon calculations for 1,3-cyclopentadiene and 3-penten-1-yne obtained from [41]. The weighted sum of both isomers

fits the measured PIE curve of the doped flame well at a HAB of 4.5 mm and predicts a ratio of 75:25. The onsets match the ionization potentials.

There are five possible C_4H_2O isomers whose ionization energies and PIE curves were calculated by Kasper et al. [42]. The Franck-Condon simulations of two possible isomers (HCCCHCO and H_2CCCCO) and the measured PIE curve are shown in Fig. 9. The small onset at about 8.61 eV could be caused by H_2CCCCO, which has a calculated adiabatic ionization energy of 8.66 eV. The next onset fits the most stable C_4H_2O isomer [42], HCCCHCO, that can be formed by reaction of diacetylene with OH radical [43]. The species assignment is therefore different from [42] where H_2CCCCO was the most likely isomer in a THF flame. The identification can help to understand the oxidation pathways of small polyynes under fuel-rich conditions.

4. Conclusions

A slightly sooting, premixed flat acetylene flame with a stoichiometry of ϕ = 2.4 at low pressure (40 mbar) was investigated by MBMS in combination with VUV photoionization at the ALS and the SLS. The effect of ethanol addition to the neat acetylene flame was studied with regard to soot precursors. Ethanol addition results in a decrease of the soot precursor propargyl (C3H3), benzene (C6H6), and the polyynes. From the reduction of soot precursor concentration, a degradation of soot due to the addition of ethanol can be inferred. Otherwise, the addition of ethanol leads to an increase of oxygenated hydrocarbons like aldehydes.

Mole-fraction profiles of over 50 species were calculated and compared with initial modeling results. The good agreement for major species and several intermediate species confirms the high quality of the presented data set. These experimental results give a detailed survey of the flame structure and can help to improve future kinetic models.

Acknowledgments

TB and TK are grateful for financial support from MIWF. All measurements were performed at the ALS and the SLS, respectively. The Advanced Light Source is supported by the Director, Office of Science, Office of Basic Energy Sciences, of the U.S. Department of energy under Contract No. DE-AC02-05CH11231. The work was financially supported by the Swiss Federal Office for Energy (BFE Contract Number 101969/152433). AL is supported by the US Department of Energy, Office of Basic Energy Sciences (BES) under Grand No. DE-SC0001198 (the Combustion Energy Frontier Research Center). We appreciate support and helpful discussions from Nils Hansen, Phil Westmoreland, Katharina Kohse-Höinghaus and all other members of the ALS and SLS flame team.

References

[1] M. Balat, H. Balat, *Appl. Energy* 86 (2009) 2273-2282.

[2] C. Esarte, Á. Millera, R. Bilbao, M.U. Alzueta, *Ind. Eng. Chem. Res.* 49 (2010) 6772-6779.

[3] I.E. Gerasimov, D.A. Knyazkov, S.A. Yakimov, T.A. Bolshova, A.G. Shmakov, O.P. Korobeinichev, *Combust. Flame* 159 (2012) 1840-1850.

[4] D. Golea, Y. Rezgui, M. Guemini, S. Hamdane, *J. Phys. Chem. A* 116 (2012) 3625-3642.

[5] M.M. Maricq, *Combust. Flame* 159 (2012) 170-180.

[6] M. Frenklach, *Phys. Chem. Chem. Phys.* 4 (2002) 2028-2037.

[7] H. Böhm, A. Lamprecht, B. Atakan, K. Kohse-Höinghaus, *Phys. Chem. Chem. Phys.* 2 (2000) 4956-4961.

[8] H. Richter, J.B. Howard, *Prog. Energy Combust. Sci.* 26 (2000) 565-608.

[9] A.V. Krestinin, *Combust. Flame* 121 (2000) 513-524.

[10] C. Yao, X. Yang, R.R. Raine, C. Cheng, Z. Tian, Y.Li, *Energy Fuels* 23 (2009) 3543-3548.

[11] C. Douté, J.-L. Delfau, C. Vovelle, *Combust. Sci. and Tech.* 103 (1994) 153-173.

[12] A. Lamprecht, B. Atakan, K. Kohse-Höinghaus, *Combust. Flame* 122 (2000) 483-491.

[13] P.R. Westmoreland, *Experimental and theoretical analysis of oxidation and growth chemistry in a fuel-rich acetylene flame*, PhD thesis, Massachusetts Institute of Technology, Cambridge, USA, 1986.

[14] R. Ancia, P.J. Van Tiggelen, J. Vandooren, *Exp. Therm. Fluid Sci.* 28 (2004) 715-722.

[15] Y. Li, L. Zhang, Z. Tian, T. Yuan, K. Zhang, B. Yang, F. Qi, *Proc. Combust. Inst. 32* (2009) 1293-1300.

[16] P.R. Westmoreland, W. Li, N. Hansen, T. Kasper, T.A. Cool, A. Lucassen, K. Kohse-Höinghaus, *Proceedings of the 6th US National Combustion Meeting* 3 (2009) 1401-1406.

[17] T. Kasper, U. Struckmeier, P. Oßwald, K. Kohse-Höinghaus, *Proc. Combust. Inst.* 32 (2009) 1285-1292.

[18] N. Hansen, T.A. Cool, P.R. Westmoreland, K. Kohse-Höinghaus, *Prog. Energy Combust. Sci.* 35 (2009) 168-191.

[19] P. Oßwald, P. Hemberger, T. Bierkandt, E. Akyildiz, M. Köhler, A. Boedi, T. Gerber, T. Kasper, *Rev. Sci. Instrum.* (Accepted 2013).

[20] A. Bodi, P. Hemberger, T. Gerber, B. Sztaray, *Rev. Sci. Instrum.* 83 (2012) 083105.

[21] A. Bodi, M. Johnson, T. Gerber, Z. Gengeliczki, B. Sztaray, T. Baer, *Rev. Sci. Instrum.* 80 (2009) 034101.

[22] T.A. Cool, K. Nakajima, C.A. Taatjes, A. Mcllroy, P.R. Westmoreland, M.E. Law, A. Morel, *Proc. Combust. Inst.* 30 (2005) 1681-1688.

[23] N.J. Labbe V. Seshadri, T. Kasper, N. Hansen, P. Oßwald, P.R. Westmoreland, *Proc. Combust. Inst.* 34 (2013) 259-267.

[24] C.A. Taatjes, N. Hansen, J.A. Miller, T.A. Cool, J. Wang, P.R. Westmoreland, M.E. Law, T. Kasper, K. Kohse-Höinghaus, *J. Phys. Chem. A* 110 (2006) 3254-3260.

[25] N. Hansen, J.A. Miller, T. Kasper, K. Kohse-Höinghaus, P.R. Westmoreland, J. Wang, T.A. Cool, *Proc. Combust. Inst.* 32 (2009) 623-630.

[26] H. Richter, J.B. Howard, *Phys. Chem. Chem. Phys.* 4 (2002) 2038-2055.

[27] J.D. Savee, S. Soorkia, O. Welz, T.M. Selby, C.A. Taatjes, D.L. Osborn, *J. Chem. Phys.* 136 (2012) 134307.

[28] P. Botschwina, R. Oswald, *Chem. Phys.* 378 (2010) 4-10.

[29] P. Hemberger, M. Lang, B. Noller, I. Fischer, C. Alcaraz, B.K. Cunha de Miranda, G.A. Garcia, H. Soldi-Lose, *J. Phys. Chem. A* 115 (2011) 2225-2230.

[30] C.L. Rasmussen, M.S. Skjoth-Rasmussen, A.D. Jensen, P. Glarborg, *Proc. Combust. Inst.* 30 (2005) 1023-1031.

[31] H. Wang, M. Frenklach, *Combust. Flame* 110 (1997) 173-221.

[32] N. Hansen, S.J. Klippenstein, C.A. Taatjes, J.A. Miller, J. Wang, T.A. Cool, B. Yang, R. Yang, L. Wei, C. Huang, J. Wang, F. Qi, M.E. Law, P.R. Westmoreland, *J. Phys. Chem. A* 110 (2006) 3670-3678.

[33] S. Soorkia, A.J. Trevitt, T.M. Selby, D.L. Osborn, C.A. Taatjes, K.R. Wilson, S.R. Leone, *J. Phys. Chem. A* 114 (2010) 3340-3354.

[34] T.A. Cool, J. Wang, K. Nakajima, C.A. Craig, A. Mcllroy, *Int. J. Mass Spectrom.* 247 (2005) 18-27.

[35] G. Blanquart, P. Pepiot-Desjardins, H. Pitch, *Combust. Flame* 156 (2009) 588-607.

[36] A.V. Krestinin, M.B. Kislov, A.V. Raevskii, O.I. Kolesova, L.N. Stesik, *Kinet. Catal.* 41 (2000) 90-98.

[37] T. Schüßler, H.-J. Deyerl, S. Dümmler, I. Fischer, C. Alcaraz, *J. Chem. Phys.* 118 (2003) 9077-9080.

[38] C.A. Taatjes, S.J. Klippenstein, N. Hansen, J.A. Miller, T.A. Cool, J. Wang, M.E. Law, P.R. Westmoreland, *Phys. Chem. Chem. Phys.* 7 (2005) 806-813.

[39] N. Hansen, S.J. Klippenstein, P.R. Westmoreland, T. Kasper, K. Kohse-Höinghaus. J. Wang, T.A. Cool, *Phys. Chem. Chem. Phys.* 10 (2008) 366-374.

[40] R.I. Kaiser, B.J. Sun, H.M. Lin, A.H.H. Chang, A.M. Mebel, O. Kostko, M. Ahmed, *Astrophys. J.* 719 (2010) 1884-1889.

[41] N. Hansen, S.J. Klippenstein, J.A. Miller, J. Wang, T.A. Cool, M.E. Law, P.R. Westmoreland, T. Kasper, K. Kohse-Höinghaus, *J. Phys. Chem. A* 110 (2006) 4376-4388.

[42] T. Kasper, A. Lucassen, A.W. Jasper, W. Li, P.R. Westmoreland, K. Kohse-Höinghaus, B. Yang, J. Wang, T.A. Cool, N. Hansen, *Z. Phys. Chem.* 225 (2011) 1237-1270.

[43] J.P. Senosiain, S.J. Klippenstein, J.A. Miller, *Proc. Combust. Inst.* 31 (2007) 185-192.

Figures

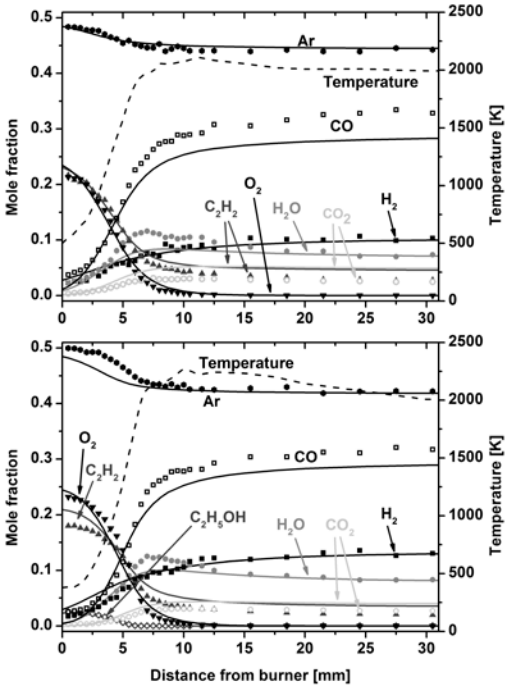

Figure 1. Temperature profiles and mole fraction profiles of the major species in the pure acetylene flame (top) and in the acetylene flame doped with ethanol (bottom). Symbols: experiment, lines: modeling.

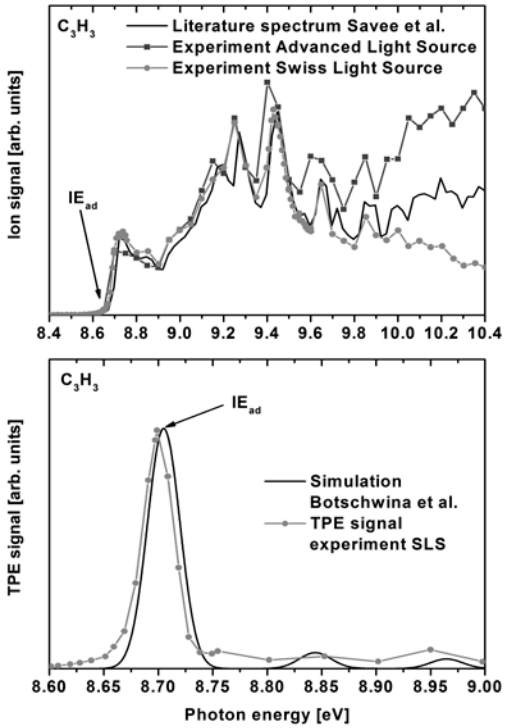

Figure 2. PIE (top) and mass-selected TPE spectra (bottom) of the propargyl radical measured in an acetylene flame compared to a literature spectra and a Franck-Condon Simulation, respectively.

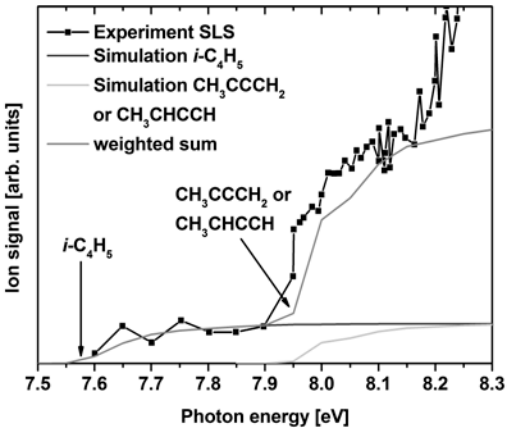

Figure 3. Comparison of Franck-Condon simulation for photoionization of C_4H_5 isomers from [32] with experimental data obtained from acetylene flame measurements at the SLS.

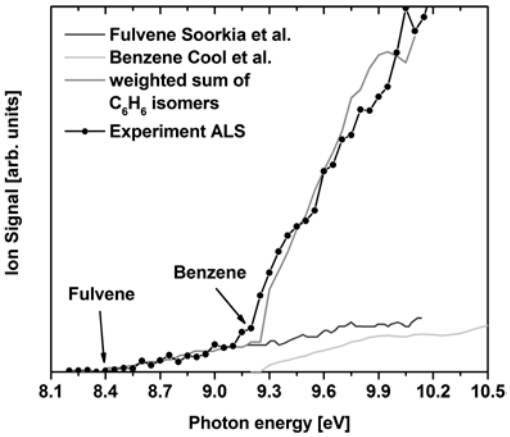

Figure 4. Identification of benzene and fulvene in the pure acetylene flame by comparison of literature cross sections between 8.2 and 10.2 eV with the measured PIE curve.

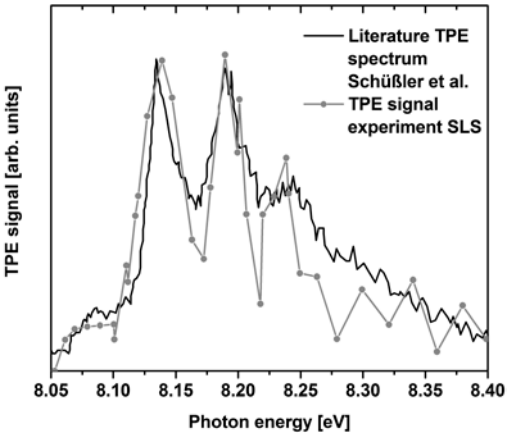

Figure 5. Identification of allyl radical in the acetylene flame by threshold photoelectron spectroscopy.

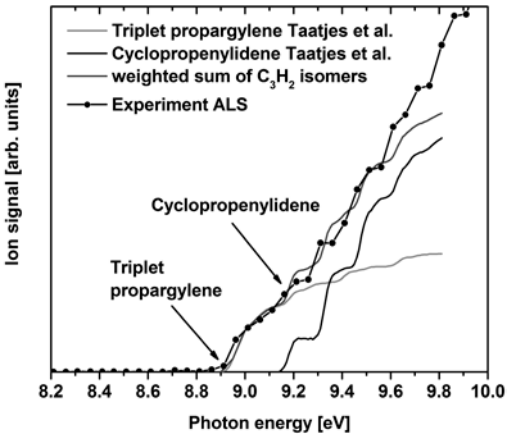

Figure 6. Identification of C_3H_2 isomers in the pure acetylene flame by comparison of Franck-Condon simulations with the measured PIE curve.

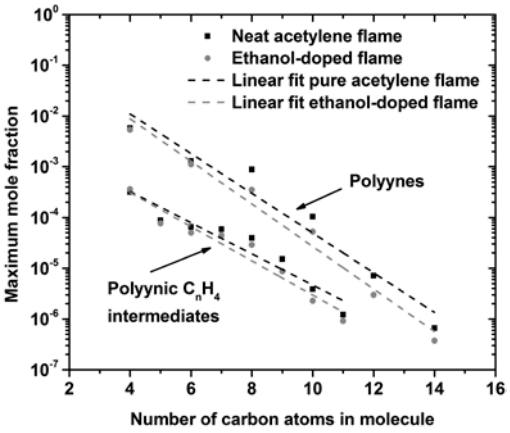

Figure 7. Maximum mole fractions of polyynes and polyyinic C_nH_4 intermediates in fuel-rich acetylene and ethanol-doped flame measured at the ALS.

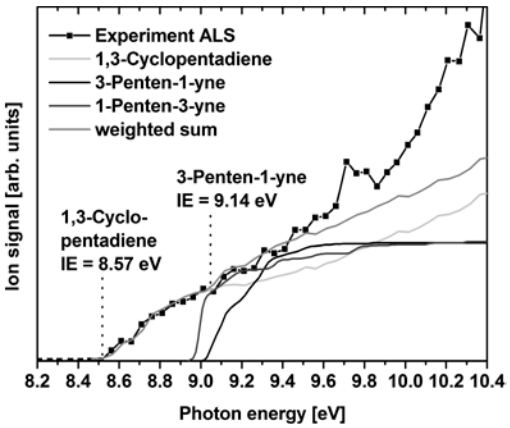

Figure 8. Comparison of PIE curve for m/z = 66 (C_5H_6) from the ethanol-doped flame to Franck-Condon simulations of C_5H_6 isomers from [41].

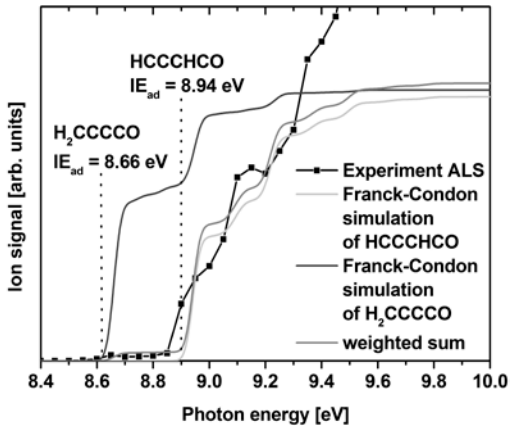

Figure 9. Comparison of experimental PIE curve from pure acetylene flame measured at 6.5 mm to the Franck-Condon simulations of C_4H_2O isomers from [42].

List of figure captions:

Figure 1. Temperature profiles and mole fraction profiles of the major species in the pure acetylene flame (top) and in the acetylene flame doped with ethanol (bottom). Symbols: experiment, lines: modeling.

Figure 2. PIE (top) and mass-selected TPE spectra (bottom) of the propargyl radical measured in an acetylene flame compared to a literature spectra and a Franck-Condon Simulation, respectively.

Figure 3. Comparison of Franck-Condon simulation for photoionization of C_4H_5 isomers from [32] with experimental data obtained from acetylene flame measurements at the SLS.

Figure 4. Identification of benzene and fulvene in the pure acetylene flame by comparison of literature cross sections between 8.2 and 10.2 eV with the measured PIE curve.

Figure 5. Identification of allyl radical in the acetylene flame by threshold photoelectron spectroscopy.

Figure 6. Identification of C_3H_2 isomers in the pure acetylene flame by comparison of Franck-Condon simulations with the measured PIE curve.

Figure 7. Maximum mole fractions of polyynes and polyyinic C_nH_4 intermediates in fuel-rich acetylene and ethanol-doped flame measured at the ALS.

Figure 8. Comparison of PIE curve for m/z = 66 (C_5H_6) from the ethanol-doped flame to Franck-Condon simulations of C_5H_6 isomers from [41].

Figure 9. Comparison of experimental PIE curve from pure acetylene flame measured at 6.5 mm to the Franck-Condon simulations of C_4H_2O isomers from [42].